



## Effect of Zincate Treatment of As-Cast AZ91 Mg Alloy on Electrodeposition of Copper in a Copper Pyrophosphate Bath

Nguyen Van Phuong<sup>a</sup>, Min-Sik Park<sup>b</sup>, Chang Dong Yim<sup>a,c</sup>, Bong Sun You<sup>a,c</sup>,  
Sungmo Moon<sup>a,c,\*</sup>

<sup>a</sup>Korea Institute of Materials Science, Gyeongnam 51508, Republic of Korea

<sup>b</sup>KMW Inc., Gyeonggi 18462, Korea

<sup>c</sup>Korea University of Science and Technology, Daejeon 34113, Korea

(Received September 13, 2016 ; revised October 27, 2016 ; accepted October 27, 2016)

### Abstract

In this work, effect of zincate treatment of AZ91 Mg alloy on the following electrodeposition of copper was examined in a non-cyanide bath containing pyrophosphate ions in view of surface morphology and adhesion of the electrodeposited copper layer. Without zincate treatment, the electrodeposited copper layer showed very porous structure and poor adhesion. On the other hand, the copper layer electrodeposited on the zincate-treated surface showed dense structure and good adhesion. The dissolution rate of AZ91 Mg alloy after the zincate treatment appeared to decrease about 40 times in the copper pyrophosphate bath, as compared to that of the surface without zincate treatment. The porous morphology and poor adhesion of a copper layer on the AZ91 Mg alloy surface without zincate treatment were attributed to small number of nucleation sites of copper because of rapid dissolution of the magnesium substrate in the pyrophosphate bath. Based on the experimental results, it is concluded that the zincate treatment to form a conducting and protecting layer on the AZ91 Mg alloy surface is essential for successful electrodeposition of a copper layer on AZ91 Mg alloy with good adhesion and dense structure in the copper pyrophosphate bath.

*Keywords* : Mg alloy, Copper plating, Electroplating, AZ91 Mg alloy, Pyrophosphate, Zincate treatment.

### 1. Introduction

In recent years, many surface treatments have been developed for corrosion protection of magnesium alloys such as chemical conversion coatings, plasma electrolytic oxidation coating, anodization, electrochemical plating, organic coating and metal coating [1-6]. Among them, plasma electrolytic oxidation, anodization treatments and organic coatings are popular processes that significantly improve the corrosion resistance of Mg alloys [1,7-9]. In some applications, the formation of conductive coatings on Mg alloys which can protect Mg alloys from corrosion is required [3]. The

metallic coatings formed by electro- or electroless platings have been explored on Mg alloys to provide not only conductive nature but also better corrosion resistance [3,10,11]. However, there are several problems of plating on Mg alloys [1,3,10,12]: (1) Mg rapidly reacts with plating solution to dissolve Mg<sup>2+</sup> ions into solution, which decreases the life time of the plating bath, especially for the electroless bath; (2) the high electrical resistance of the surface films, which is formed spontaneously on the Mg alloy surface, inhibit successive electrodeposition of metallic layer; (3) different activities of phases ( $\alpha$ -phase and  $\beta$ -phase) in Mg alloys may result in non-uniform deposition of metallic coatings.

Several metals have been chosen for electrodeposition on Mg alloy such as copper, nickel, chromium into a single layer or multilayer coatings [3,10]. Among them, electroplating of copper can be highly

\*Corresponding Author : Sungmo Moon

Korea Institute of Materials Science, Korea University of Science and Technology  
Tel : +82-55-280-3549 ; Fax: +82-55-280-3570  
E-mail : [sungmo@kims.re.kr](mailto:sungmo@kims.re.kr)

valuable in applications such as the manufacturing of electronic parts and components, as well as products used in the aerospace and defense industries [12,13]. Copper has excellent electrical conductivity which is making it more effective than other materials for use as an electrical component. Copper also provides superior protection against corrosion in comparison to other metals and it has been widely studied on Mg alloys [12,14-21]. However, if the copper layer contains any imperfections, such as pinhole, crack or non-deposited surface, corrosion of the Mg alloy surface can be extremely increased because of galvanic coupling effect between large area of copper cathode and small area of magnesium anode. Thus, it is quite important to deposit a copper layer without such imperfections.

There are three basic types of copper electroplating baths: acid copper bath, alkaline cyanide copper bath and alkaline noncyanide copper bath [13,14]. The electrodeposition of copper from acid baths is used extensively for electroforming, electrorefining and decorative electroplating. The acid copper process is low-cost, easy to control and highly efficient in deposition. However, the use of acid baths is not suitable on Mg alloys because of a problem of fast Mg dissolution in acidic solutions. Alkaline cyanide copper process is the most often used method which is easily controlled process to produce thin deposit of relatively uniform thickness throughout the metal-finishing industry for many applications. However it is being restricted because of their toxicity and waste treatment problem. Thus, alkaline noncyanide copper plating method has been the subject of recent interest primarily due to environmental issue and disposal of cyanide-containing processes [14-21].

Alkaline copper pyrophosphate baths offer a number of desirable features. The copper pyrophosphate plating baths operate at nearly 100% deposition efficiency and provide good throwing power, and also, they are non-corrosive because operating solution pH is near neutral. Copper pyrophosphate baths have been used to deposit copper onto zinc die castings, steel and aluminum [13,21]. However, the copper pyrophosphate bath can hardly be used for Mg alloys because pyrophosphate ions can rapidly react with Mg and  $\text{Mg(OH)}_2$  to form dissolvable complexes  $[\text{Mg}_2(\text{P}_2\text{O}_7)_x]^{4-4x}$ , which can decrease not only adhesion of electrodeposited copper layer but also the life time of plating bath. Therefore, to plate copper on Mg alloys in pyrophosphate solution, Lee et al. [22] added very high concentration of  $\text{F}^-$  ions into plating

solution to form stable film of  $\text{Mg(OH)}_x\text{F}_{2-x}$  on the surface which prevents the dissolution of Mg alloy. However,  $\text{Mg(OH)}_x\text{F}_{2-x}$  film had high electrical resistance which can inhibit the electroplating of copper. Kato et al. [23] used copper cyanide bath for strike electroplating and then copper pyrophosphate bath for thickening of electrodeposited copper layer. However, still there is lack of information on how to achieve good adhesion and uniform thickness of electrodeposited layer without pinhole defects on AZ91 Mg alloy in a copper pyrophosphate bath.

In the present study, uniform thickness and good adhesion of electrodeposited copper layer have been achieved on AZ91 Mg alloy in a copper pyrophosphate bath by employing appropriate zincate treatment process before the copper electroplating. The effects of zincate treatment on dissolution of AZ91 Mg alloy and adhesion of electrodeposited copper layer were studied in a copper pyrophosphate bath and the copper layer electrodeposited on the zincate-treated AZ91 Mg alloy surface was characterized in terms of surface morphology, surface roughness and coating thickness.

## 2. Experimental

AZ91 Mg alloy with composition (wt. %) of Al, 8.88; Zn, 0.73; Mn, 0.196; Si < 0.02; Fe, < 0.01; Cu, < 0.01; Ni, < 0.005; and Mg balance, was used a substrate for copper electrodeposition in this study. The samples with a size of 50 mm × 25 mm × 2 mm were cut from an as-cast ingot. The samples were ground in ethanol using SiC abrasive papers successively up to 2000 grit, rinsed with ethanol and then dried with a compressed air. The bath compositions and operation conditions for the pretreatments and electroplating of copper in a noncyanide copper pyrophosphate solution are given in Table 1. The surface and cross-sectional morphologies were observed by an optical microscope (OM, Hirox, Japan). Photographs showing the surface appearances of electroplated samples were taken using a Canon S95 digital camera. The weight of AZ91 sample with and without zincate treatment was first measured before immersion and then it was measured again after immersion for 1 min in the copper pyrophosphate bath at OCP (open-circuit potential) and 55°C and removing a Cu layer deposited by galvanic displacement. The Cu layer was removed in an aqueous solution containing  $\text{NH}_4\text{OH}$  (28 vol.%) and  $\text{H}_2\text{O}_2$  (35 vol.%) at R.T. for 1 min. Weight loss of AZ91 Mg alloy during

Table 1. Bath compositions and operation conditions for pretreatments and electrodeposition of copper on AZ91 Mg alloy.

| Process            | Bath composition   | Concentration (mol/L) | Condition                                    |
|--------------------|--|-----------------------|--|
| (a) SiC-abrading   |  |                       | up to #2000 grit                             |
| (b) Activation     | HF   | 0.5                   | 0.5 min                                      |
| (c) Zincating      | ZnSO <sub>4</sub> ·7H <sub>2</sub> O                             | 0.2                   | pH 10.3, 60°C, 10 min                        |
|                    | K <sub>4</sub> P <sub>2</sub> O <sub>7</sub>                     | 0.42                  |  |
|                    | Na <sub>2</sub> CO <sub>3</sub>                                  | 0.05                  |  |
|                    | KF   | 0.1                   |  |
| (d) Copper plating | Cu <sub>2</sub> P <sub>2</sub> O <sub>7</sub> ·3H <sub>2</sub> O | 0.2                   | pH 8.0, Temp. 55°C,<br>10 mA/cm <sup>2</sup> |
|                    | K <sub>4</sub> P <sub>2</sub> O <sub>7</sub>                     | 0.9                   |  |
|                    | C <sub>6</sub> H <sub>5</sub> K <sub>3</sub> O <sub>7</sub>      | 0.08                  |  |

immersion at OCP in the copper pyrophosphate bath was calculated from the weights measured.

The surface roughness of the coating was measured by SurfTest SJ-400 (Mitutoyo, Japan). The adhesion of the electrodeposited copper layer was tested by tape test method according to ASTM D3359 standard [24]. The coated samples were scratched both vertically and horizontally, with a tool holding 11 cutting blades, with 1 mm separation from each other; thus leaving 100 small squares of 1 mm<sup>2</sup> area. A strip of adhesive tape was applied to the scratched surface with a constant pressure, and then pulled off at an angle 90° to the plate surface for the adhesion test.

### 3. Results and Discussion

Figure 1 presents optical microscopy images of AZ91 Mg alloy after SiC-abrading and zincate treatment. Scratch lines induced from mechanical polishing step were observed on the SiC-abraded AZ91 surface (Fig. 1(a)), but they became almost invisible after the zincate treatment (Fig. 1(b)), indicating a significant dissolution of AZ91 Mg alloy during the zincating process. After the zincate treatment in Fig. 1(b), two different phases of AZ91, primary α-Mg and second β-Mg<sub>17</sub>Al<sub>12</sub> phase, became clearly visible. Both α- and β-phases were found to be fully covered with zincate layers after 10 min of zincate treatment. The observation of the α- and β-phases after the zincate treatment is explained by their different dissolution rates during activation in HF solution and different deposition rates during zincate treatment, which arise from the different open-circuit potentials (OCP) of the α- and β-phases [3,7,12]. The deposition of zinc on Mg alloys in the zincate solution is expressed by three main reactions [12,19].

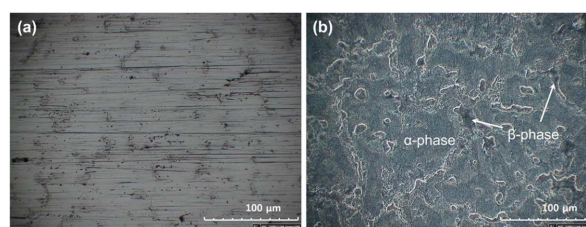
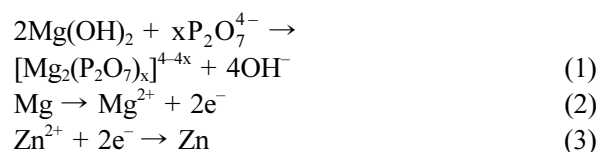


Fig. 1. Optical microscopy images of AZ91 Mg alloy after (a) SiC-abrading and (b) zincate treatment.



Due to higher OCP potential of the β-phase (-1.3 V vs. SHE) than that of the α-phase (-1.6 V vs. SHE), the deposition of zinc occurs first on the cathodic site (β-phase) rather than that on the anodic site (α-phase) [12]. Therefore, the zincate layer formed on the β-phase could be thicker than that on the α-phase as indicated by darker color of zincate on the β-phase than the α-phase.

Figure 2 displays optical microscopy images obtained before and after tape test of copper layers electrodeposited for 10 min on AZ91 Mg alloy without and with zincate treatment for 10 min. Without zincate treatment, Fig. 2(a) shows that the electrodeposited copper layer is porous and does not fully cover the AZ91 Mg alloy surface. The electrodeposited copper layer formed without the zincate treatment showed poor adhesion, as confirmed by its easy detachment after tape test (Fig. 2(c)). In contrast, the electrodeposited copper layer on the sample with zincate treatment was denser without any pores or defects (Fig. 2(b)), and had good adhesion without any detachment of the copper layer

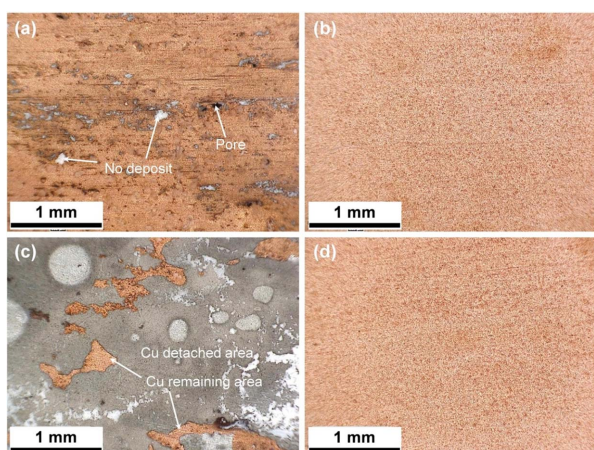


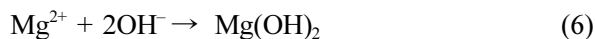
Fig. 2. Optical microscopy images obtained (a, b) before and (c, d) after tape test of copper layer electrodeposited for 10 min on AZ91 Mg alloy (a, c) without and (b, d) with zincate treatment.

after the tape test (Fig. 2(d)). The porous structure and poor adhesion of the electrodeposited copper layer on non-zincated surface can be explained by small number of nucleation sites for copper electrodeposition due to the presence of non-conductive  $Mg(OH)_2$  films and fast dissolution of AZ91 Mg alloy.

The deposition of copper occurred by both an external source of current and galvanic displacement reaction between Mg and  $Cu^{2+}$ :



and  $Mg(OH)_2$  can be formed together with the deposition of copper layer:



In the pyrophosphate solution, Mg can form  $Mg(OH)_2$  through reactions (2) and (6), and  $Mg(OH)_2$  can quickly react with pyrophosphate ions as described by reactions (1). Considering that  $Mg^{2+}$  ions are not stable in alkaline solution, it is reasonable to conclude that repeating of the formation and dissolution reactions of  $Mg(OH)_2$  is primary dissolution step of Mg, instead of direct dissolution of Mg into  $Mg^{2+}$  ions in the copper pyrophosphate bath.

Without zincate treatment, the dissolution rate of AZ91 Mg alloy was much higher, about 40 times, compared with the zincated surface (Table 2). The rapid dissolution of Mg through  $Mg(OH)_2$  into

Table 2. Weight loss of AZ91 Mg alloy with and without zincate treatment after 1 min immersion at OCP in copper pyrophosphate solution at 55°C.

| Without zincate treatment<br>( $mg\ cm^{-2}$ ) | With zincate treatment<br>( $mg\ cm^{-2}$ ) |
|--|---|
| 2.3±0.1  | 0.06±0.004                                  |

electroplating solution can decrease the life time of electroplating bath and also induce the presence of porous  $Mg(OH)_2$  with a high electrical resistance on the surface, which decreased the number of nucleation sites for copper deposition. On the other hand, zincate-treated AZ91 Mg alloy showed very low dissolution rate in the pyrophosphate bath (Table 1 2), which is ascribed to the presence of a protective zincate layer on the surface as verified already in Fig. 1 (b). Since the zincate layer not only reduces the dissolution of Mg alloy but also provides nucleation sites for copper electrodeposition, the electrodeposited copper layer after zincate treatment has denser structure and better adhesion than that of non-zincate treated surface.

Figure 3 shows the surface appearances of electrodeposited copper layer on AZ91 Mg alloy obtained with the electrodeposition time after zincate treatment. All the surfaces showed bright and homogenous color of copper, irrespective of electrodeposition time. There were no visible pores or defects in the copper layer electrodeposited after the zincate treatment. The surface images of these four samples were observed in more detail by optical microscope and the results are presented in Fig. 4. After 5 min of electrodeposition time, preferential electrodeposition of copper on  $\beta$ -phase in AZ91 alloy is noticeable in Fig. 4(a), which may arise from the microscopically non-uniform deposition of zincate layer on the surfaces of  $\alpha$ - and the  $\beta$ - phases in AZ91 alloy. Different OCP values of the  $\alpha$ - and  $\beta$ -phases may affect the asymmetric deposition of Cu

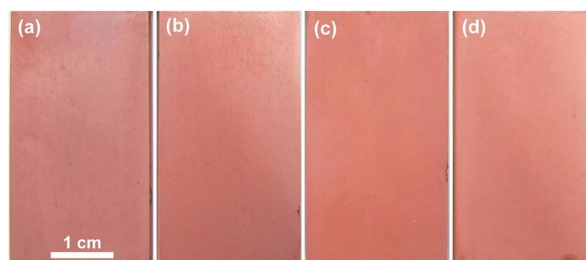


Fig. 3. Photographs of electrodeposited copper layers on AZ91 Mg alloy obtained at 10  $mA\ cm^{-2}$  for (a) 5 min, (b) 20 min, (c) 40 min and (d) 60 min in copper pyrophosphate solution after zincate treatment.



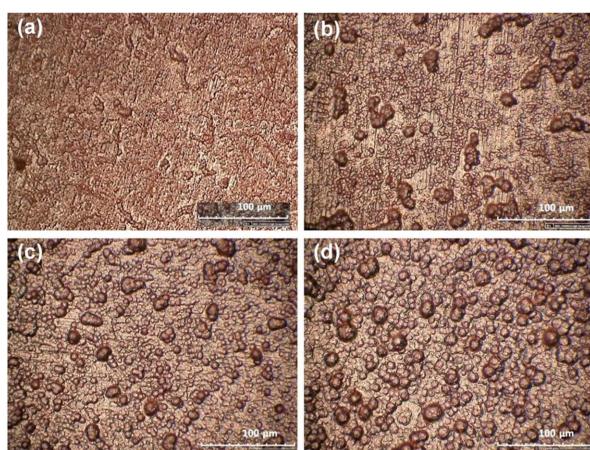


Fig. 4. Optical-microscopy images of electrodeposited copper layer on AZ91 Mg alloy obtained at 10 mA cm<sup>-2</sup> after zincate treatment with various Cu deposition times of (a) 5 min, (b) 20 min, (c) 40 min and (d) 60 min.

on the α- and β-phases.

It is interesting to note that preferential growth of a copper layer on the β- phase disappears and the formation of nodular surface structure became noticeable after 20 min of electrodeposition. The size of nodules appeared to increase with copper electrodeposition time from about 8 μm at 40 min to about 12 μm at 60 min of electroplating time. Although the formation of nodules is commonly obtained on copper electroplating [25,26], still their formation mechanism seems to be very complex. At present, several factors have been suggested to explain the formation mechanisms of nodular structure of a copper layer, such as anode sludge, the morphology of the substrate and the operation parameters such as pH, temperature, ion concentrations and current density [25,26].

The scratched lines formed during mechanical polishing step were still visible on the electrodeposited surfaces for 5 min (Fig. 4(a)) and 20 min (Fig. 4(b)), suggesting the formation of very thin copper layer and no removal of scratches due to slight dissolution of the alloy surface during the zincate and electro-deposition processes. With increasing the deposition time to 30 min, both scratched lines disappeared, implying the deposition of a thick copper layer.

Changes in thickness of the electrodeposited copper layer on AZ91 Mg alloy with plating time were investigated by the observation of cross-sectional views in Fig. 5. After 5 min of deposition time, thin copper layers with non-uniform thickness were formed on the surface (Fig. 5(a)). However after 20 min of deposition, the electrodeposited copper layer became thick to about 4 - 5 μm and

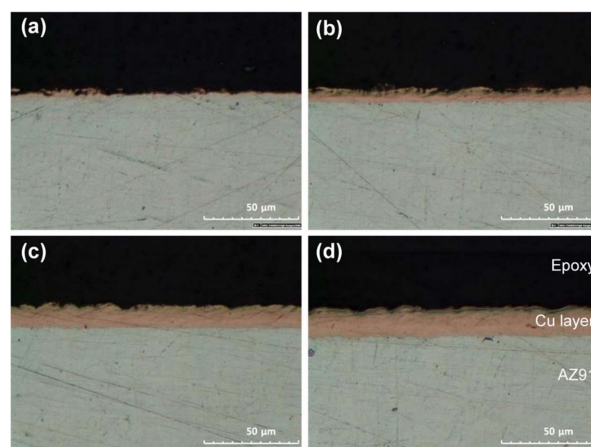


Fig. 5. Cross-sectional views of electrodeposited copper layer on AZ91 Mg alloy obtained at 10 mA cm<sup>-2</sup> after zincate treatment with various Cu deposition times of (a) 5 min, (b) 20 min, (c) 40 min and (d) 60 min.

covered the whole AZ91 surface uniformly. The thickness increased to about 10 μm after 40 min and about 15 μm after 60 min of electrodeposition time, suggesting that the deposition rate of a copper layer is about 0.25 μm/min at an applied cathodic current density of 10 mA/cm<sup>2</sup> in the copper pyrophosphate bath.

It should be pointed out that the electrodeposited copper layer on AZ91 in the pyrophosphate bath is much thicker and more uniform in thickness than a copper layer electrodeposited in a copper cyanide solution. Without an activation treatment, the electrodeposited copper layer in the cyanide solution showed non-uniform thickness on α- and β- phases, ranging from 5 to 10 μm [12]. Uniform thickness of a copper layer in the cyanide solution was achieved after an activation treatment in 0.5 M HF solution for zincate treatment in a previous work [12]. The copper cyanide solution is typically used for strike plating with the maximum thickness of several μm. Thus, it is concluded that the copper pyrophosphate bath can be used for the formation of thicker and more uniform layer of copper on AZ91 Mg alloy, compared to the cyanide bath.

Figure 6 demonstrates the surface roughness of electrodeposited copper layer on AZ91 Mg alloy with electrodeposition time. The initial surface roughness, Ra, of zincated AZ91 was about 0.5 μm and the surface increased up to about 1.0 μm after 10 min and about 1.7 μm after 60 min of electrodeposition time. The increased surface roughness is explained by the growth of nodules with deposition time as discussed in Fig. 4.

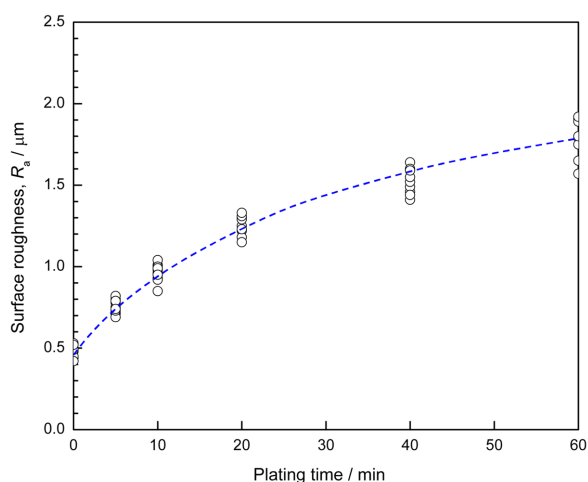


Fig. 6. Surface roughness of electrodeposited copper layer on AZ91 Mg alloy with electrodeposition time at  $10 \text{ mA cm}^{-2}$  after zincate treatment.

The adhesion of copper layer on AZ91 Mg alloy with different electrodeposition times was assessed by tape test according to ASTM D3359 [24] and the results were given in Fig. 7. It was observed that the electrodeposited copper layer on AZ91 Mg alloy after zincate treatment exhibits good adhesion with no detachment of copper flakes, irrespective of the electrodeposition time. Comparing with the adhesion of electrodeposited copper layer on the non-zincate treated surface in Fig. 2, the adhesion of electrodeposited copper layer on zincated AZ91 is much better. This confirms that the zincate treatment is a key step for improving the adhesion of electrodeposited copper layer. The questions how to identify the

quality of successful zincate treatment and how the zincate treatment time affects the deposition process and adhesion of the electrodeposited copper layer will be discussed in a following paper.

#### 4. Conclusions

In this work, effect of zincate treatment on the copper electrodeposition on AZ91 Mg alloy was investigated in a copper pyrophosphate bath. Without the zincate treatment, loosely bonded porous copper layer was obtained on the AZ91 Mg alloy surface under the application of cathodic current, and dissolution of AZ91 Mg alloy occurred fast in the copper pyrophosphate bath. The poor adhesion of Cu layer on the AZ91 Mg alloy surface without zincate treatment is attributed to small number of nucleation sites of copper on the substrate due to rapid dissolution reaction between the substrate and pyrophosphate solution. The zincate treatment decreased the dissolution rate of AZ91 Mg alloy about 40 times. Electrodeposited copper layer on AZ91 Mg alloy after an appropriate zincate treatment showed good adhesion and uniform thickness with bright surface appearance, independent of the deposition time. The surface roughness of the electrodeposited copper layer was found to increase with increasing Cu deposition time due to the formation of nodular surface structure. The deposition rate of copper was obtained to be about  $0.25 \mu\text{m}/\text{min}$  at a current density of  $10 \text{ mA}/\text{cm}^2$ .

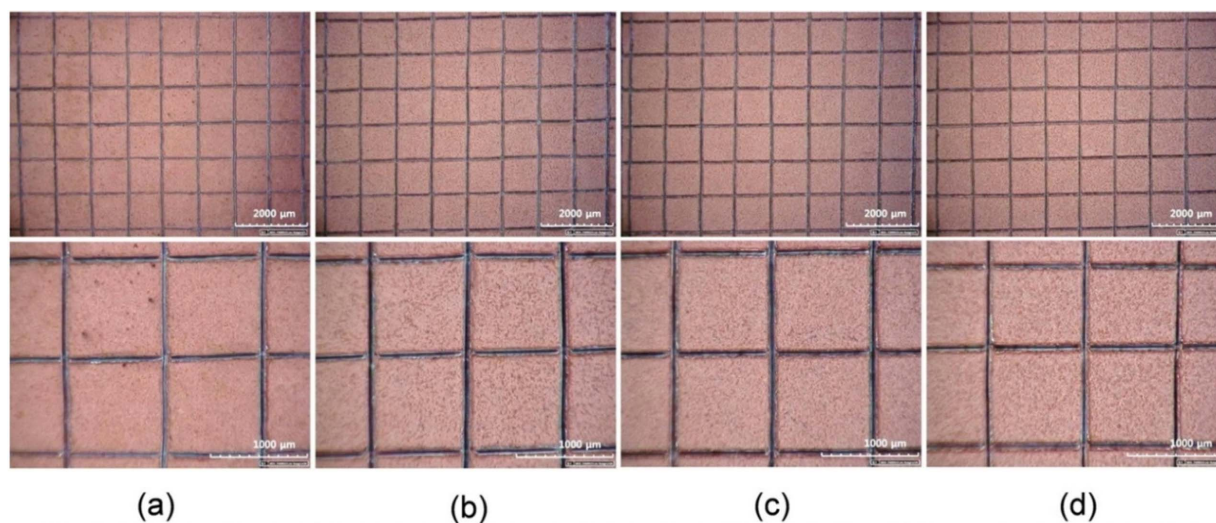


Fig. 7. Optical microscopy images obtained at different magnifications after tape test of electrodeposited copper layer on AZ91 Mg alloy at  $10 \text{ mA cm}^{-2}$  after zincate treatment with various Cu electrodeposition times of (a) 5 min, (b) 20 min, (c) 40 min and (d) 60 min.

### Acknowledgment

This research was financially supported by a research grant of WC 300 R&D program from the Ministry of Trade, Industry and Energy (MOTIE) (PGM8660).

### References

- [1] J. E. Gray, B. Luan, Protective coatings on magnesium and its alloys – a critical review, *J. Alloy Compd.*, 336 (2002) 88-113.
- [2] N. V. Phuong, K. H. Lee, D. Chang, M. Kim, S. Lee, S. Moon, Zinc phosphate conversion coatings on magnesium alloys – a review, *Met. Mater. Int.*, 19 (2013) 273-281.
- [3] X. B. Chen, H. Y. Yang, T. B. Abbott, M. A. Easton, N. Birbilis, Corrosion-resistance electrochemical platings on magnesium alloys: A state-of-the-art review, *Corrosion*, 68 (2011) 518-535.
- [4] G. L. Song, Corrosion prevention of magnesium alloys, Woodhead Publishing Limited. (2013).
- [5] R. F. Basit, S. Moon, Formation of cerium conversion coatings on AZ31 magnesium alloy, *J. Kor. Inst. Surf. Eng.*, 49 (2016) 1-13.
- [6] F. Czerwinski, Magnesium alloys – Corrosion and surface treatments, InTech, Croatia, (2011) 153-184.
- [7] T. S. N. Sankara Narayanan, I. S. Park, M. H. Lee, Strategies to improve the corrosion resistance of microarc oxidation (MAO) coated magnesium alloys for degradable implants: Prospects and challenges, *Prog. Mater. Sci.*, 60 (2014) 1-71.
- [8] N. V. Phuong, S. Moon, Deposition and characterization of E-paint on magnesium alloys, *Prog. Org. Coat.*, 89 (2015) 91-99.
- [9] A. Atrens, G. -L. Song, M. Liu, Z. Shi, F. Cao, M. S. Dargusch, Review of recent developments in the field of magnesium corrosion, *Adv. Eng. Mater.*, 17 (2015) 400-453.
- [10] L. P. Wu, J. J. Zhao, Y. P. Xie, Z. D. Yang, Progress of electroplating and electroless plating on magnesium alloy, *Trans. Nonferrous Met. Soc. China*, 20 (2010) 630-637.
- [11] X. P. Lei, G. Yu, Y. P. Zhu, Z. P. Zhang, X. M. He, B. N. Hu, Y. Chen, Successful cyanide free plating protocols on magnesium alloys, *T. I. Met. Finish.*, 88 (2010) 75-80.
- [12] N. V. Phuong, M. S. Park, C. D. Yim, B. S. You, S. Moon, Electrodeposition of copper on AZ91 Mg alloy in cyanide solution, *J. Kor. Inst. Surf. Eng.*, 49 (2016) 238-244.
- [13] Modern electroplating 5<sup>th</sup> edition, Mordechay Schlesinger (Editor), Milan Paunovic (Editor), A John Wiley & Sons, Inc., Publication (2010) 33-78.
- [14] C. A. Huang, T. H. Wang, T. Weirich, V. Neubert, A pretreatment with galvanostatic etching for copper electrodeposition on pure magnesium and magnesium alloys in an alkaline copper-sulfate bath, *Electrochim. Acta*, 53 (2008) 7235-7241.
- [15] P. Zhu, L.Y. Wang, G.R. Qian, T.H. Cao, Copper coating electrodeposited directly onto AZ31 magnesium alloy, *Anti-Corros. Method. M.*, 60 (2013) 127-133.
- [16] J. Tang, K. Azumi, Effect of copper pretreatment on the zincate process and subsequent copper electrodeposition of AZ31 magnesium alloy, *J. Electrochem. Soc.*, 158 (2011) D535-D540.
- [17] P. Zhu, L. Y. Wang, Y. Chen, M. Zhou, J. Zhou, Electrodeposition of copper coating on AZ31 magnesium alloy, *Surf. Eng.*, 28 (2012) 796-799.
- [18] J. C. Ballesteros, E. Chainet, P. Ozil, Y. Meas, G. Trejo, Electrodeposition of copper from non-cyanide alkaline solution containing tartrate, *Int. J. Electrochem. Sci.*, 6 (2011) 2632-2651.
- [19] J. Tang, K. Azumi, Influence of zincate pretreatment on adhesion strength of a copper electroplating layer on AZ91 D magnesium alloy, *Surf. Coat. Tech.*, 205 (2011) 3050-3057.
- [20] C. A. Huang, Y. H. Yeh, C. K. Lin, C. Y. Hsieh, Copper electrodeposition on a magnesium alloy (AZ80) with a U-Shaped surface, *Materials*, 7 (2014) 7366-7378.
- [21] O. Radovici, Cecilia Vass, I. Solacolu, Some aspects of copper electrodeposition from pyrophosphate electrolytes, *Electrodepos. Surface Treat.*, 2 (1974) 263-273.
- [22] J. H. Lee, Y. H. Kim, U. C. Jung, W. S. Chung, Electroplating on magnesium alloy in KF-added pyrophosphate copper bath, *Kor. J. Met. Mater.*, 48 (2010) 218-224.
- [23] J. Kato, W. Urushihara, T. Nakayama, Magnesium based alloys article and a method thereof, US Patent No: 6,068,938.
- [24] ASTM standard D3359-02, ASTM International; 2004, 06.01.
- [25] Tohru Watanabe, Nano-plating: Microstructure control theory of plated film and data base of plated film microstructure, Elsevier (2004).
- [26] M. Hayase, Electronics Packaging 3, The Electrochemical Society (2009).